

# Effects of Monascin on Anti-inflammation Mediated by Nrf2 Activation in Advanced Glycation End Product-Treated THP-1 Monocytes and Methylglyoxal-Treated Wistar Rats

Bao-Hong Lee,<sup>†</sup> Wei-Hsuan Hsu,<sup>†</sup> Tao Huang,<sup>†</sup> Yu-Ying Chang,<sup>†</sup> Ya-Wen Hsu,<sup>§</sup> and Tzu-Ming Pan<sup>\*,†</sup>

<sup>†</sup>Department of Biochemical Science and Technology, College of Life Science, National Taiwan University, No. 1, Sec. 4, Roosevelt Road, Taipei 10617, Taiwan

<sup>§</sup>SunWay Biotechnology Company, Taipei, Taiwan

**S** Supporting Information

**ABSTRACT:** Hyperglycemia is associated with advanced glycation end products (AGEs). This study was designed to evaluate the inhibitory effects of monascin on receptor for advanced glycation end product (RAGE) signal and THP-1 monocyte inflammation after treatment with S100b, a specific ligand of RAGE. Monascin inhibited cytokine production by S100b-treated THP-1 monocytes via up-regulation of nuclear factor-erythroid 2-related factor-2 (Nrf2) and alleviated p47phox translocation to the membrane. Methylglyoxal (MG, 600 mg/kg bw) was used to induce diabetes in Wistar rats. Inhibitions of RAGE and p47phox by monascin were confirmed by peripheral blood mononuclear cells (PBMCs) of MG-induced rats. Silymarin (SM) was used as a positive control group. It was found that monascin promoted heme oxygenase-1 (HO-1) expression mediated by Nrf2. Suppressions of AGEs, tumor necrosis factor- $\alpha$  (TNF- $\alpha$ ), and interleukin-1 $\beta$  (IL- $\beta$ ) in serum of MG-induced rats were attenuated in the monascin administration group treated with retinoic acid (RA). RA treatment resulted in Nrf2 inactivation by increasing RA receptor- $\alpha$  (RAR $\alpha$ ) activity, suggesting that RA acts as an inhibitor of Nrf2. The results showed that monascin exerted anti-inflammatory and antioxidative effects mediated by Nrf2 to prevent the development of diseases such as type 2 diabetes caused by inflammation.

**KEYWORDS:** monascin, receptor for advanced glycation end product, methylglyoxal, silymarin, nuclear factor-erythroid 2-related factor-2, retinoic acid receptor- $\alpha$

## INTRODUCTION

Hyperglycemia is associated with protein glycation; advanced glycation end products (AGEs) are generated by the non-enzymatic interaction between carbohydrates and proteins.<sup>1–3</sup> AGEs have properties to generate free radicals and undergo autoxidation to generate other reactive intermediates, thereby resulting in the development of diabetes.<sup>4</sup> Methylglyoxal (MG) is a highly reactive dicarbonyl metabolite produced during glucose metabolism<sup>5</sup> and is a major precursor of AGEs involved in the pathogenesis of diabetes and inflammation. Studies suggest that AGEs and MG can generate large amounts of pro-inflammatory cytokines through receptor for AGEs (RAGE) activation, and these results are related to the modulation of inflammatory molecules through oxidative stress.<sup>5–8</sup>

Recently, several types of foods and drinks, including coffee, cream, and cake, have been known to result in high MG levels in the plasma, thus causing both nutritional and health concerns. Coffee has been reported to contain a high level of MG of 230  $\mu$ M (17.7 mg/L).<sup>9</sup> In addition, approximately 5100  $\mu$ g/g of MG was determined in honey.<sup>10</sup> In Spain, dietary exposures of the Spanish population to glyoxal and MG from cookies were estimated to be 213 and 216  $\mu$ g/person/day, respectively.<sup>11</sup> Wine and beer were found to have 1556 and 1000  $\mu$ g/L MG, respectively.<sup>12,13</sup> Plasma of diabetic patients contains a high level of MG (200  $\mu$ g/L) when compared to that of a nondiabetic human (5  $\mu$ g/L).<sup>14</sup> These suggest that MG

from dietary foods is accumulated in the plasma in nondiabetic humans and the level may be equal to diabetic patients.

Various antioxidants have been evaluated for their ability to activate nuclear factor-erythroid 2-related factor 2 (Nrf2) to attenuate oxidative damage by promoting heme oxygenase-1 (HO-1), including quercetin and phenolic acid.<sup>15,16</sup> In addition, a previous study reported that an antioxidant (silymarin) inhibited AGE generation, thereby improving diabetes.<sup>17</sup> Several flavonoids have also been reported to suppress inflammation by inhibiting RAGE signal in THP-1 cells.<sup>18</sup> RAGE activation is related to the modulation of signaling molecules such as p47phox to result in oxidative stress.<sup>19</sup> S100b is a calcium-binding protein expressed and secreted by astrocytes. S100b can activate RAGE<sup>20,21</sup> and induce reactive oxygen species (ROS) overproduction<sup>22</sup> and protein kinase C (PKC) phosphorylation,<sup>23</sup> thereby resulting in inflammation.

Monascin is a major anti-inflammatory compound identified from *Monascus*-fermented products. In addition, monascin has been reported to possess cytotoxic/cytostatic<sup>24</sup> and anti-inflammatory activities,<sup>25</sup> rephrase to avoid immunosuppressive activity on mouse T splenocytes.<sup>26</sup> We previously demonstrated that monascin regulated adipogenesis and lipolysis in 3T3-L1

**Received:** November 27, 2012

**Revised:** January 17, 2013

**Accepted:** January 18, 2013

**Published:** January 20, 2013

cells, suggesting antiobesity potential.<sup>27</sup> In addition, monascin can activate peroxisome proliferator activated receptor- $\gamma$  (PPAR $\gamma$ ) to improve insulin resistance in C2C12 cells.<sup>28</sup> In a recent study, we also found that monascin elongated the life span of *Caenorhabditis elegans* mediated by antioxidation and improved hyperglycemia in streptozotocin-induced rats.<sup>29</sup>

Retinoic acid (RA) shows inhibitory activity toward Nrf2 through activation of retinoic acid receptor- $\alpha$  (RAR $\alpha$ ).<sup>30</sup> However, the anti-inflammatory and antidiabetic mechanisms of monascin in AGE-induced rats and THP-1 cells are both unknown. In the present study, we investigated the inhibition of RAGE signal by monascin up-regulation of Nrf2 in THP-1 cells to confirm whether this anti-inflammatory effect was associated with Nrf2 in MG-induced rats. Moreover, Nrf2 siRNA transfection and RA administration were used in vitro and in vivo for Nrf2 inhibition.

## MATERIALS AND METHODS

**Chemicals.** Monascin was isolated from *Monascus*-fermented rice (red mold rice).<sup>31</sup> Glucose, dichlorofluorescein diacetate (DCFH-DA), retinoic acid, methylglyoxal (MG), and lipopolysaccharides (LPS) were purchased from Sigma-Aldrich (St. Louis, MO, USA). The anti-Nrf2 antibody for rat was purchased from Bioss Inc. (Woburn, MA, USA). Anti-p47phox antibody for human/rat, anti-RAGE antibody for human, anti-Keap-1 antibody for human, and anti-RAR $\alpha$  antibody for rat were purchased from Santa Cruz Biotechnology Inc. (Burlingame, CA, USA). Anti-Nrf2 antibody, anti-lamin B antibody, anti-NF $\kappa$ B antibody, anti-p-PKC antibody for human, and anti-GAPDH antibody for human/rat were purchased from Epitomics Inc. (Burlingame, CA, USA). Anti-Nrf2 antibody for rat was purchased from Bioss Inc. Fetal bovine serum was purchased from Hyclone (Logan, UT, USA). RPMI 1640 medium, L-glutamine, sodium pyruvate, and antibiotics (penicillin/streptomycin) were purchased from Gibco (Grand Island, NY, USA).

**Cell Culture.** THP-1, a human monocytic leukemia cell line, was obtained from the Bioresource Collection and Research Center (BCRC 60430; Food Industry Research and Development Institute, Hsinchu, Taiwan). Cells were maintained in RPMI 1640 medium supplemented with 10% FBS, streptomycin (100 mg/mL), penicillin (100 U/mL), 50  $\mu$ M  $\beta$ -mercaptoethanol, and 5.5 mM D-glucose in a 5% CO<sub>2</sub> incubator at 37 °C. S100b is a peptide produced mostly by astroglial cells; S100b can activate RAGE and produce inflammatory mediators in monocytes. For RAGE activation experiments, S100b protein (10  $\mu$ g/mL), a specific RAGE ligand, was given to cells for 8 or 12 h with or without monascin (5–50  $\mu$ M). Monascin had no cytotoxicity on THP-1 monocytes at a concentration range of 5–50  $\mu$ M (cell viability > 87%; Supporting Information Supplementary Figure 1). Silymarin (SM), which has been reported to show antiglycation, anti-inflammatory, and antidiabetes activities,<sup>11</sup> was used as a positive control in the current study.

**ROS Measurement.** The level of oxidative stress was monitored by the measurement of ROS. Collected cells were suspended in 500  $\mu$ L of PBS and mixed with 10  $\mu$ M (final concentration) DCFH-DA to incubate for 20 min at 37 °C. The cells were washed three times with PBS to remove redundant DCFH-DA. The cell pellet was mixed with 500  $\mu$ L of PBS, and the ROS level was assayed by flow cytometry (Becton-Dickinson, San Jose, CA, USA).<sup>32</sup>

**Assay for Inflammatory Cytokines.** Cytokines (TNF- $\alpha$  and IL-1 $\beta$ ) in THP-1 culturing medium and serum were measured by ELISA kits purchased from Peprotech (Rocky Hill, NJ, USA).

**Nuclear Protein Extraction of THP-1.** Nuclear protein extraction from THP-1 monocytes or PBMCs was obtained according to the kit protocol supplied by the manufacturer (Fermentas, Life Sciences, Burlington, ON, Canada).

**Nrf2 Knockdown of THP-1 Cells by Specific siRNA.** Nrf2 interference of THP-1 cells was performed with lipofectamine RNAiMAX transfection reagent followed by the protocols provided (Invitrogen, Carlsbad, CA, USA). The sequence of specific small

interfering RNA (siRNA) for Nrf2 was designed (5' CCA ACC AGU UGA CAG UGA ACU CAU U3' and 5' AAU GAG UUC ACU GUC AAC UGG UUG G3'), and the control group was transfected with scramble siRNA. Cell lysates were subjected to Western blotting with anti-Nrf2 antibody to confirm the inhibition of Nrf2 expression.

**Nrf2-ARE Reporter Assay.** A DNA fragment containing three copies of the antioxidant response element-4 (ARE4) from glutamate-cysteine ligase (GCL) gene (5'-CCC GTG ACT CAG CGC TCC GTG ACT CAG CGC TCC GTG ACT CAG CGC T-3') was subcloned into a pGL3-promoter vector to construct pGL3-ARE4-Luc. THP-1 monocytes were transiently transfected with a DNA mixture containing 2  $\mu$ g of pGL3-ARE4-Luc and 0.5  $\mu$ g of control plasmid pRL-TK (Promega, Madison, WI, USA) using the transfection reagent (Invitrogen, Carlsbad, CA, USA). At 24 h following transfection, the cells were treated with monascin or SM for various times. Whole-cell lysates were prepared, and luciferase activity was conducted utilizing the Dual-Luciferase kit (Promega).

**Animal Induction.** Male Wistar rats (4 weeks old) were obtained from the National Laboratory Animal Breeding and Research Center (Taipei, Taiwan). Animals were acclimatized for 1 week prior to MG induction, and they were divided at random into six treatment groups (six rats per group) and provided with food and water ad libitum. Animals were subjected to a 12 h light/dark cycle with a maintained relative humidity of 60% and a temperature at 25 °C (protocol complied with guidelines described in the "Animal Protection Law", amended on January 17, 2001, Hua-Zong-(1)-Yi-Tzi-9000007530, Council of Agriculture, Executive Yuan, Taiwan, ROC). The animal study was approved by the Institutional Animal Care and Use Committee (IACUC) of National Taiwan University. Rats were divided into the following treatment groups: (a) control (saline administration); (b) MG (600 mg/kg bw/day for 4 weeks by oral administration); (c) MG + monascin (10 mg/kg bw/day for 4 weeks by oral administration); (d) MG + SM (10 mg/kg bw/day for 4 weeks by oral administration); (e) MG + monascin + retinoic acid (RA, 10 mg/kg bw/day for 4 weeks by intraperitoneal injection); (f) MG + SM + RA groups. After induction, animals were sacrificed by CO<sub>2</sub> asphyxia to carry out the following assays.

**AGEs and Inflammatory Factors Measurements.** The AGEs (Cee Biolabs, Inc., Beverly, MA, USA), TNF- $\alpha$  (eBioscience, San Diego, CA, USA), and IL-1 $\beta$  (Peprotech, Rocky Hill, NJ, USA) ELISA kits were purchased to measure the levels in serum.

**Peripheral Blood Mononuclear Cells (PBMCs) Identification and Culture.** Blood of animal was collected and centrifuged at 4 °C (250g) for 20 min; in turn, serum was collected, and red blood cells (RBC) in the cell pellet were lysed by RBC lysis buffer. After centrifugation (4 °C, 250g) for 5 min, the peripheral blood mononuclear cells (PBMCs) were collected. These cells were separated into three portions for (a) RNA extraction by Trizol for vascular cell adhesion molecule-1 (VCAM-1) mRNA measurements (Life Technologies, Carlsbad, CA, USA), (b) protein extraction by cell lysis buffer (Cell Signaling Technology) for p47phox assay by Western blot, and (c) cell culture. PBMCs (5  $\times$  10<sup>6</sup> in 60 mm dish) were incubated in RPMI 1640 medium supplemented with 10% FBS, streptomycin (100 mg/mL), penicillin (100 U/mL), 50  $\mu$ M  $\beta$ -mercaptoethanol, and 25 mM D-glucose in a 5% CO<sub>2</sub> incubator at 37 °C. Monascin (25  $\mu$ M), SM (25  $\mu$ M), or RA (25  $\mu$ M) was given to cells for 8 h of treatment. Subsequently, the cell protein was extracted to measure nuclear Nrf2 and RAR $\alpha$  levels of PBMCs by Western blot, and HO-1 and GCL mRNA expression were measured by real-time PCR.

**Real-Time PCR.** The reverse transcription product was diluted in water, and a volume corresponding to 30 ng of original RNA was used for real-time PCR. Real-time PCR amplification and detection were performed using SYBR Green. Primers: human GAPDH, 5'-ACC AGC CTC AAG ATC ATC AGC A-3' (forward) and 5'-TGC TAA GCA GTT GGT GGT GC-3' (reverse); human HO-1, 5'-ATG GCC TCC CTG TAC CAC ATC-3' (forward) and 5'-TGT TGC GCT CAA TCT CCT CCT-3' (reverse); human GCL, 5'-TGC AGT TGA CAT GGC CTG TT-3' (forward) and 5'-TCA CAG AAT CCA GCT GTG CAA-3' (reverse); human GST, 5'-AGA GAC AGA GGA GGA

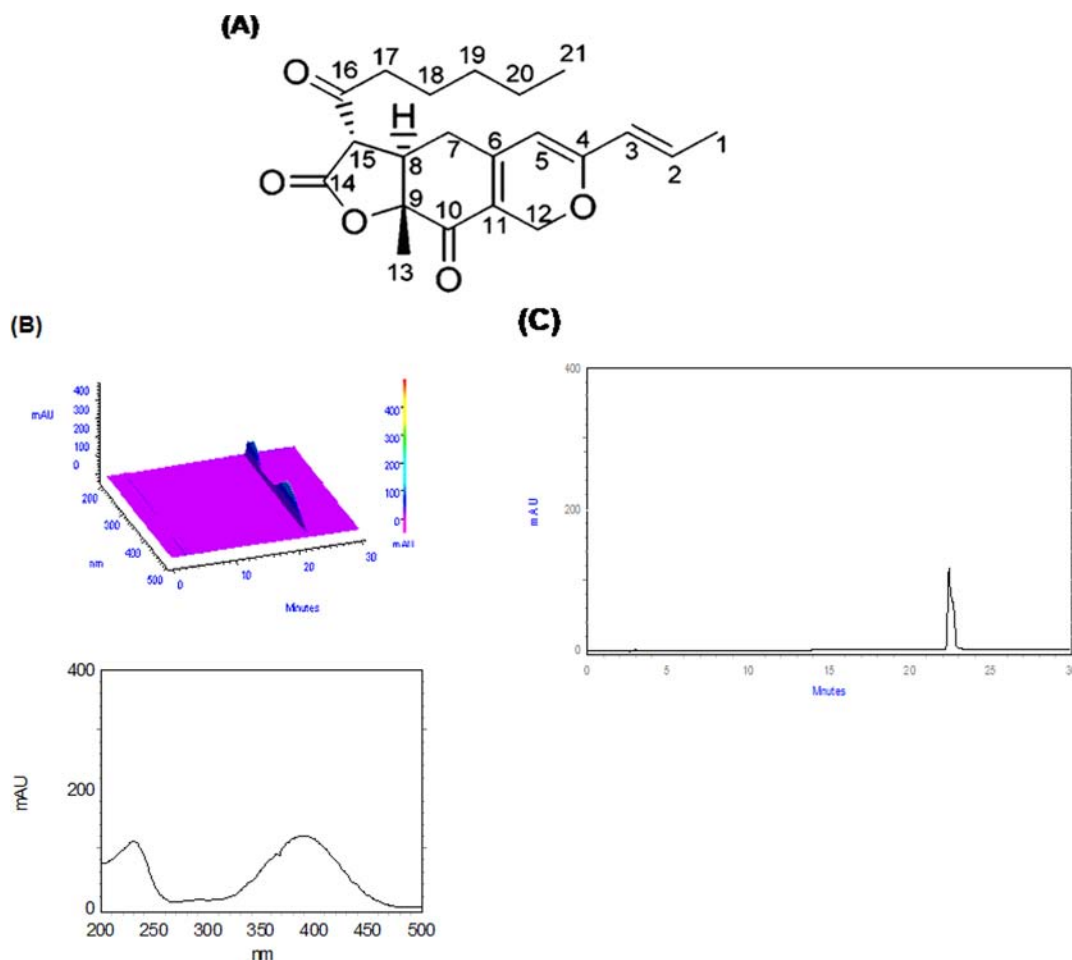


**Figure 1.** (A) Structure of monascin. Electrospray ionization mass spectrometry (ESIMS) data were  $m/z$  359  $[M + H]^+$ ;  $^1H$  NMR ( $CDCl_3$ , 200 MHz)  $\delta$  0.88 (3H, t,  $J = 6.6$  Hz, H-19), 1.30 (4H, m, H-17, H-18), 1.43 (3H, s, H-12), 1.61 (2H, m, H-16), 1.84 (3H, d,  $J = 6.0$  Hz, H-11), 2.49 (1H, m, H-15a), 2.64 (1H, m, H-5a), 2.70 (1H, m, H-15b), 2.99 (1H, m, H-5b), 3.14 (1H, m, H-6), 3.64 (1H, d,  $J = 9.0$  Hz, H-13), 4.67 (1H, d,  $J = 12.6$  Hz, H-1a), 5.02 (1H, d,  $J = 12.6$  Hz, H-1b), 5.26 (1H, s, H-4), 5.85 (1H, d,  $J = 15.4$ , H-9), 6.47 (1H, dt,  $J = 15.4, 6.0$  Hz, H-10);  $^{13}C$  NMR ( $CDCl_3$ , 50 MHz)  $\delta$  12.9 (C-19), 16.7 (C-12), 17.5 (C-11), 21.4 (C-18), 21.8 (C-16), 28.4 (C-17), 30.1 (C-5), 41.9 (C-6, C-15), 53.9 (C-13), 62.8 (C-1), 82.2 (C-7), 102.3 (C-4), 113.0 (C-8a), 123.4 (C-9), 134.4 (C-10), 149.8 (C-4a), 159.5 (C-3), 168.5 (C-13a), 188.8 (C-8), 201.5 (C-14). (B) UV spectrum of purified MS. (C) HPLC analysis of MS showed that its purity was >98%. Purified monascin was detected at 227 nm.

GCG GAT T-3' (forward) and 5'-CTG CAT GCG GTT GTC CAT-3' (reverse); rat GAPDH, 5'-ACT CCC ATT CCT CCA CCT TT-3' (forward) and 5'-TTA CTC CTT GGA GGC CAT GT-3' (reverse); rat HO-1, 5'-TCT ATC GTG CTC GCA TGA AC-3' (forward) and 5'-CAG CTC CTC AAA CAG CTC AA-3' (reverse); rat GCL, 5'-GGC AAG ATA CCT TTA TGA CCA GTT-3' (forward) and 5'-TGC AGC ACT CAA AGC CAT AA-3' (reverse); rat VCAM-1, 5'-GAG ACA AAA CAG AAG TGG AAT-3' (forward) and 5'-AGC AAC GTT GAC ATA AAG AGT-3' (reverse).

**Western Immunoblotting.** Cells were lysed in ice-cold lysis buffer containing 20 mM Tris-HCl (pH 7.4), 1% of Triton X-100, 0.1% of SDS, 2 mM EDTA, 10 mM NaF, 1 mM phenylmethanesulfonyl fluoride, 500  $\mu$ M sodium vanadate, and 10  $\mu$ g/mL aprotinin overnight. Then the cell extract was centrifuged (12000g, 10 min) to recover the supernatant. The supernatant was taken as the cell extract. The cell protein was resolved on 10% SDS-PAGE and transferred to a polyvinylidene fluoride membrane. Membranes were blocked with 5% nonfat milk for 1 h and incubated with primary antibodies for 4 h; subsequently, the membrane was washed three times each for 5 min in PBST, shaken in a solution of HRP-linked secondary antibody for 1 h, and washed three more times each for 5 min in PBST. Proteins were detected by enhanced chemiluminescent reagent (Millipore, Billerica, MA, USA).

**Statistical Analysis.** Experimental results were averaged triplicate analysis. The data were recorded as the mean  $\pm$  SD and analysis by

Statistical Analysis System (SAS Inc., Cary, NC, USA). One-way analysis of variance was performed by ANOVA procedures. Significant differences between means were determined by Duncan's multiple-range tests. Results were considered to be statistically significant at  $p < 0.05$ .

## RESULTS

**Oxidative Stress of THP-1 Treated by S100b for 12 h.** Monascin was isolated from *Monascus*-fermented rice (red mold rice). Preparation of monascin (>95% purity) is shown in Figure 1 by nuclear magnetic resonance and electrospray ionization–mass spectrometry analysis. Several studies have found that ROS production was effectively increased by S100b induction at various concentrations and durations, including 50  $\mu$ g/mL S100b treatment for 4 h,<sup>33</sup> 6.5  $\mu$ g/mL S100b treatment for 4 h,<sup>17,19,24</sup> and 10  $\mu$ g/mL S100b treatment for 8 h in THP-1 monocytes.<sup>8</sup> In addition, 1  $\mu$ g/mL S100b treatment for 5 days has been reported to induce inflammation in THP-1 monocytes.<sup>34</sup> We found that 10  $\mu$ g/mL S100b treatment significantly increased TNF- $\alpha$  in THP-1 monocytes in a time-dependent manner (Figure 2A). We found that an 8 h S100b treatment significantly increased PKC phosphorylation (Figure 2B). As shown in Figure 2C, a high ROS level was induced in



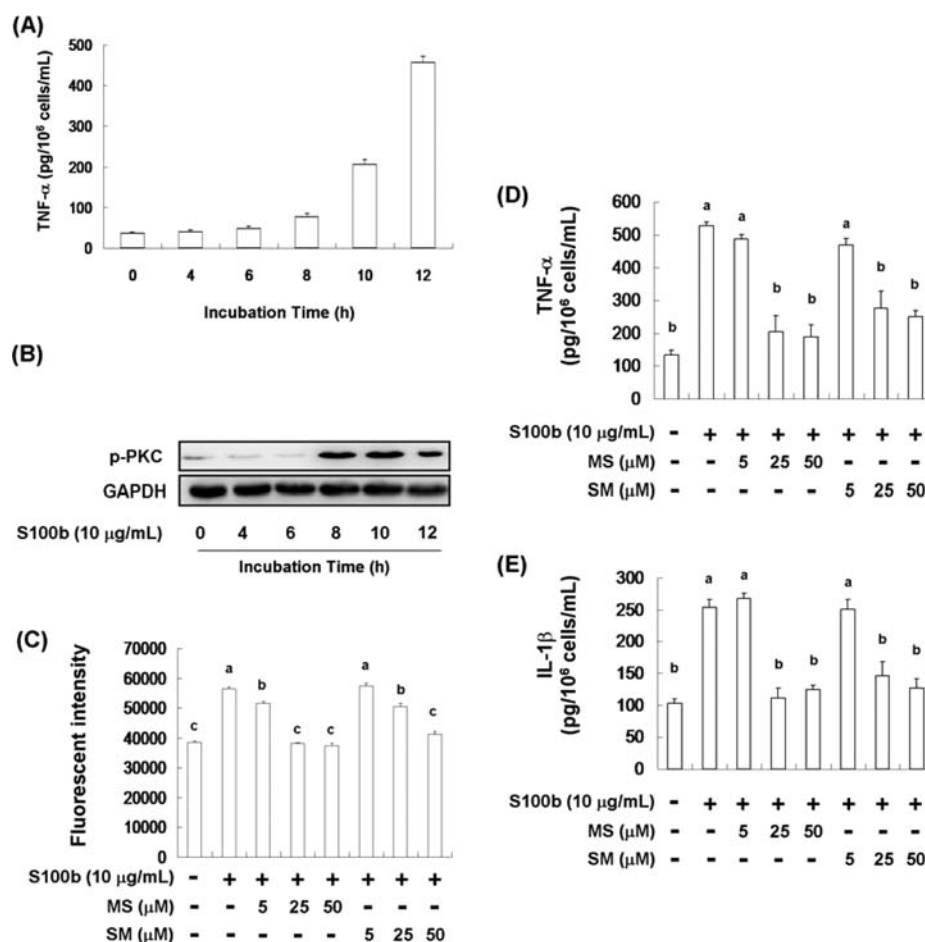


**Figure 2.** Inhibitions of monascin (MS) and silymarin (SM) on oxidative stress and inflammation. Production of TNF- $\alpha$  in THP-1 monocytes treated with S100b (10  $\mu$ g/mL) for various times was measured by ELISA kit (A). Cells were treated with S100b (10  $\mu$ g/mL) for various times, and then PKC phosphorylation was investigated by Western blot (B). In addition, THP-1 monocytes were treated by S100b (a RAGE ligand; 10  $\mu$ g/mL) with or without MS/SM (5, 25, and 50  $\mu$ M) for 12 h; subsequently, (C) intracellular ROS level was measured by DCFH-DA stain. The levels of (D) TNF- $\alpha$  and (E) IL-1 $\beta$  in culture medium were measured by ELISA kit. Data are shown as the mean  $\pm$  SD ( $n = 3$ ). Significant differences are indicated by different letters ( $p < 0.05$ ).

THP-1 monocytes by 10  $\mu$ g/mL S100b treatment for 12 h; TNF- $\alpha$  (Figure 2D) and IL-1 $\beta$  (Figure 2E) production was also increased by S100b treatment for 12 h. However, monascin and SM both significantly inhibited increases in ROS level, TNF- $\alpha$ , and IL-1 $\beta$  production induced by 12 h of S100b treatment.

**Anti-inflammatory and Antioxidative Effects of Monascin and SM.** The p-PKC level of S100b-treated THP-1 monocytes was reduced by monascin (25  $\mu$ M) and SM (25  $\mu$ M) treatment for 8 h (Figure 3A). However, neither monascin nor SM affected the RAGE expression of THP-1 cells treated with S100b for 8 h (Figure 3B). The NADPH oxidase subunit p47phox, a downstream target of the RAGE signaling pathway, was markedly translocated from the cytoplasm to the membrane of THP-1 monocytes, and its expression was also elevated after 8 h of S100b treatment. Monascin and SM were found to inhibit p47phox translocation to the membrane and lower S100b-induced p47phox expression (Figure 3C). Inflammatory factor production is regulated by nuclear factor- $\kappa$ B (NF $\kappa$ B), and their transcriptional activity is induced by p-PKC. S100b treatment for 8 h effectively elevated NF $\kappa$ B translocation from the cytoplasm into the nucleolus of THP-1 monocytes; in addition, monascin and SM both attenuated NF $\kappa$ B activation caused by S100b (Figure 3D).

Nrf2 was activated by translocation from the cytoplasm into the nucleolus.<sup>35</sup> We found that 8 h of monascin or SM treatment promoted Nrf2 nuclear translocation in S100b-induced THP-1 monocytes (Figure 3E). In addition, our results indicated that Keap-1 was elevated and Nrf2 was reduced by 8 h of S100b treatment in THP-1 monocytes, but monascin and SM treatment both attenuated Keap-1 and increased Nrf2 expression (Figure 3F).

These results suggested that Nrf2 up-regulation mediated the protective effects of monascin and SM against oxidative stress. Therefore, we investigated Nrf2 activation by monascin treatment for various durations. As shown in Figure 3G, monascin treatment began to increase nuclear Nrf2 at 4 h, and this effect was maintained at 8 h. We found that monascin markedly increased Nrf2 transcriptional activity by luciferase report assay compared with SM treatment in THP-1 monocytes (Figure 3H).

As a result, the transcription targets of Nrf2 including HO-1 and glutathione-cysteine ligase (GCL) were significantly recovered by monascin and SM treatment for 8 h compared to the S100b-induced group (Figure 4A,B). However, glutathione *S*-transferase (GST) mRNA expression was not affected by S100b, monascin, or SM treatment (Figure 4C).

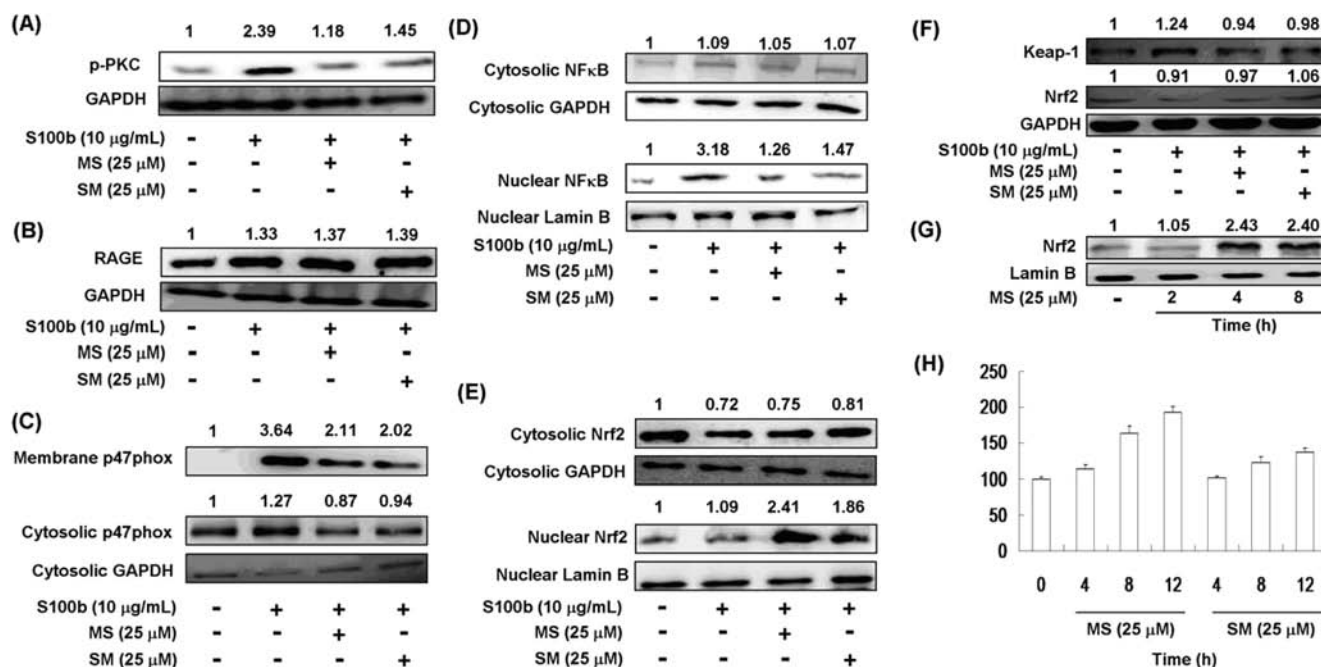


**Figure 3.** Effects of monascin (MS) and silymarin (SM) on RAGE signal and Nrf2 activation. Cells were treated by S100b (a RAGE ligand; 10 μg/mL) with or without MS/SM (25 μM) for 8 h and then measured for (A) PKC phosphorylation, (B) RAGE expression, (C) p47phox translocation, (D) NFκB translocation, (E) Nrf2 translocation, and (F) Keap-1 expression in S100b-induced THP-1 monocytes by Western blot. In addition, nuclear Nrf2 levels of THP-1 treated with MS for various times were evaluated by Western blot (G). Transcriptional activity of Nrf2 in THP-1 monocytes treated by MS and SM was investigated by luciferase reporter assay and is shown as the mean ± SD ( $n = 5$ ) (H).

**Anti-Inflammatory and Antioxidative Effects of Monascin in Nrf2-Knockdown THP-1 Monocytes.** Although monascin has been reported to exert antioxidative effects in *C. elegans* to improve insulin sensitivity,<sup>29</sup> whether these effects are related with Nrf2 activation remains unclear. To confirm the anti-inflammation of Nrf2 activation mediated by monascin, we therefore investigated the anti-inflammatory response and ROS inhibition in S100b-treated Nrf2-knockdown THP-1 monocytes. We found that 72 h of treatment with specific siRNA (50 nM) effectively interfered with Nrf2 expression of THP-1 monocytes, and a similar result was also observed in S100b-treated Nrf2-knockdown THP-1 monocytes (Figure 5A). By contrast, the inhibition of p-PKC in S100b-induced THP-1 monocytes (8 h) was attenuated in the Nrf2 siRNA groups compared to the monascin and SM treatment groups (Figure 5B).

In addition, the inhibition of oxidative stress induced by 12 h of S100b treatment was attenuated in the monascin + Nrf2 siRNA treatment group compared to the monascin treatment group. However, this result was not observed in the SM group with or without Nrf2 siRNA treatment (Figure 6A); monascin differed from SM in its demonstration of strong antioxidative activity, and the antioxidative effect of monascin was mediated by Nrf2 activation. Likewise, the inhibitory activity of 12 h of monascin treatment toward TNF-α and IL-1β in S100b-treated Nrf2-knockdown THP-1 monocytes was also abolished, and these effects were not observed in the SM treatment groups with or without Nrf2 siRNA (Figure 6B,C). The loss of antioxidative effects of monascin treatment was caused by decreases in HO-1 and GCL in S100b-treated Nrf2-knockdown THP-1 monocytes for 8 h (Figure 7).

**Anti-inflammatory and Antioxidative Effects of Monascin in MG-Induced Rats.** Rats were sacrificed after treatment with MG, monascin, SM, or RA for 4 weeks.

PBMCs were collected and treated with monascin (25 μM), SM (25 μM), or RA (25 μM) for 8 h. Subsequently, the nuclear Nrf2 level of PBMCs was measured by Western blot. As shown in Figure 8A, monascin promoted Nrf2 translocation into the nucleolus of PBMCs, and this effect was not affected in the monascin + RA treatment group compared to the monascin treatment group. Furthermore, nuclear RARα was markedly increased in PBMCs by RA administration in the monascin and SM treatment groups (Figure 8B). HO-1 and GCL mRNA expression by PBMCs in monascin + RA and SM + RA groups was also inhibited (Figure 8C,D).

**Inhibition of Serum AGEs and RAGE Signaling Molecule by Monascin in MG-Induced Rats.** AGE levels in the serum of MG-treated rats were evaluated. As shown in Figure 9A, MG significantly increased the formation and accumulation of AGEs in the serum compared with controls. However, antioxidant treatment with monascin or SM markedly suppressed this effect. We also found that RA administration may attenuate the efficacy of the inhibition of AGE production in the monascin treatment group, but this effect was not observed in SM-treated rats administered RA. Our results revealed that monascin could reduce the levels of AGEs through Nrf2 regulation. Likewise, p47phox activation was dependent on AGEs. We found that monascin markedly lowered p47phox expression of PBMCs in MG-induced rats, and this inhibition was not observed in the monascin + RA treatment group, revealing that inhibition of AGEs by monascin affected anti-inflammatory activity. However, SM treatment with or without RA administration did not affect AGEs or p47phox suppression (Figure 9B).

In addition, VCAM-1 is known to be focally elevated in atherogenesis, but we have shown the inhibition of VCAM-1 activity by monascin treatment in ovalbumin-induced THP-1 monocytes, which depended on PPAR-γ activation.<sup>36,37</sup> We

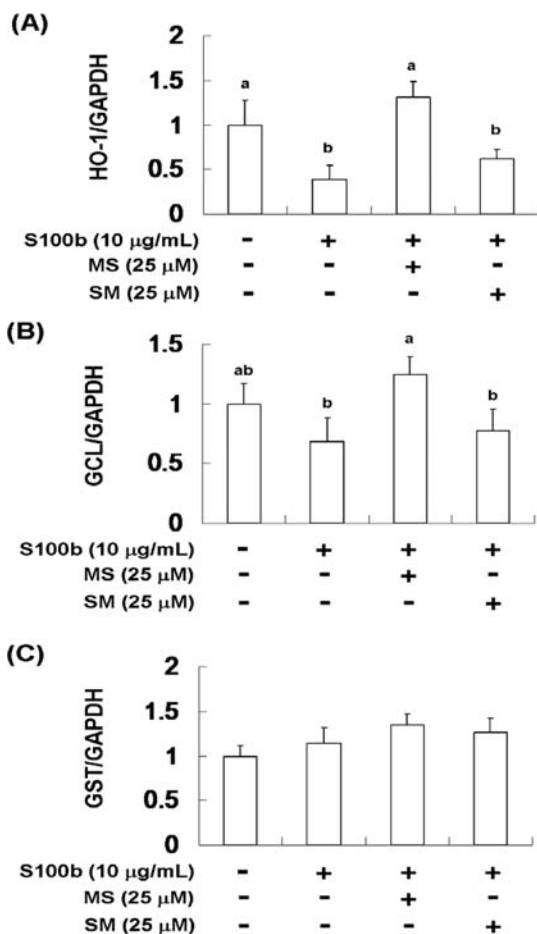


**Figure 4.** Effects of monascin (MS) and silymarin (SM) on antioxidant enzyme expression. THP-1 monocytes were treated by S100b (a RAGE ligand; 10 μg/mL) with or without MS/SM (25 μM) for 8 h, and then the mRNA expressions of (A) HO-1, (B) GCL, and (C) GST were measured by real-time PCR. Data are shown as the mean ± SD (*n* = 3). Significant differences are indicated by different letters (*p* < 0.05).

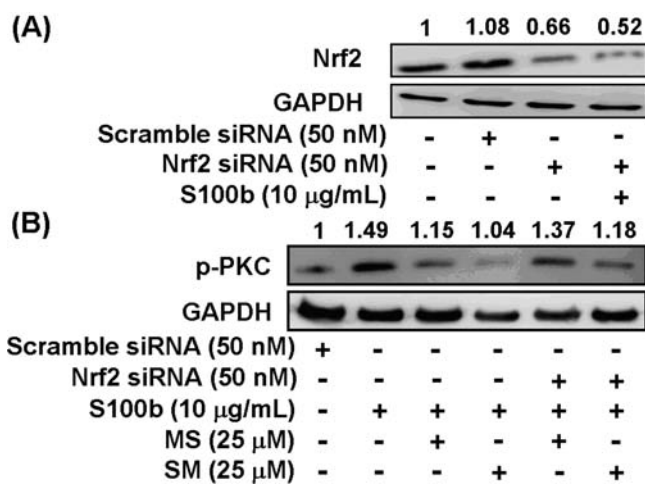


**Figure 5.** Nrf2 knockdown and PKC phosphorylation. Inhibition of Nrf2 expression in THP-1 monocytes treated with Nrf2 siRNA for 72 h was investigated (A). In addition, inhibition of PKC phosphorylation in S100b (10 μg/mL)-treated Nrf2 knockdown-THP-1 monocytes by monascin (MS; 25 μM) and silymarin (SM; 25 μM) treatment for 8 h was investigated (B).

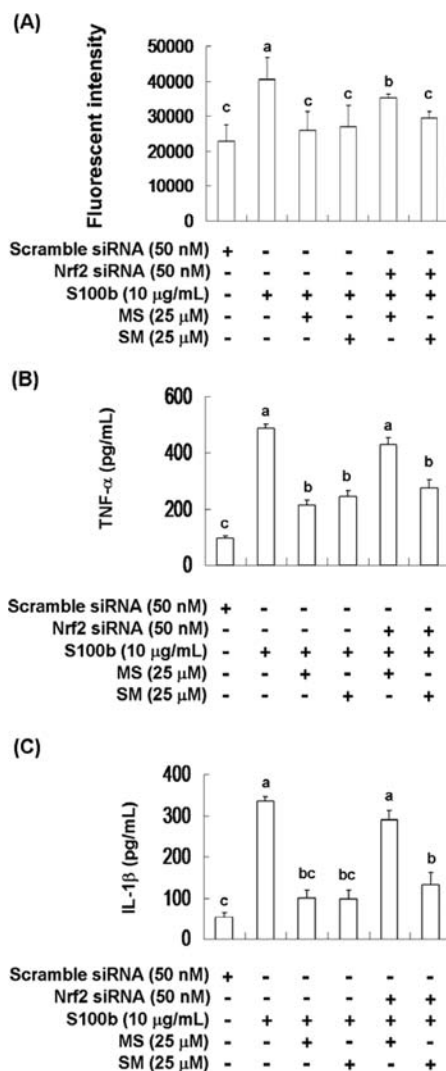


**Figure 6.** Inhibitions of monascin (MS) and silymarin (SM) on oxidative stress and inflammatory cytokines. Levels of (A) intercellular ROS, (B) TNF-α, and (C) IL-1β in culture medium of Nrf2 knockdown-THP-1 monocytes (1 × 10<sup>6</sup> cells) treated by S100b (10 μg/mL) with or without MS/SM (25 μM) for 12 h were investigated. Data are shown as the mean ± SD (*n* = 3). Significant differences are indicated by different letters (*p* < 0.05).

found that monascin and SM both inhibited VCAM-1 expression in the PBMCs of rats induced by MG; however, this inhibition was not affected by RA administration (Figure 9C).

**Anti-inflammatory Effect of Monascin in MG-Induced Rats.** RA administration did not attenuate the suppression of p47phox in PBMCs or serum AGEs from SM-treated rats; therefore, inhibition of serum TNF-α and IL-1β was not affected by SM treatment. However, suppression of serum AGEs and PBMC p47phox in monascin-administered rats was attenuated by RA treatment, resulting in the loss of anti-inflammation compared to the monascin treatment group (Figure 10A,B).

■ DISCUSSION

The contribution of protein glycation to the pathology of a number of chronic diseases such as diabetes has been well documented.<sup>5</sup> Diabetes mellitus is a complex physiological



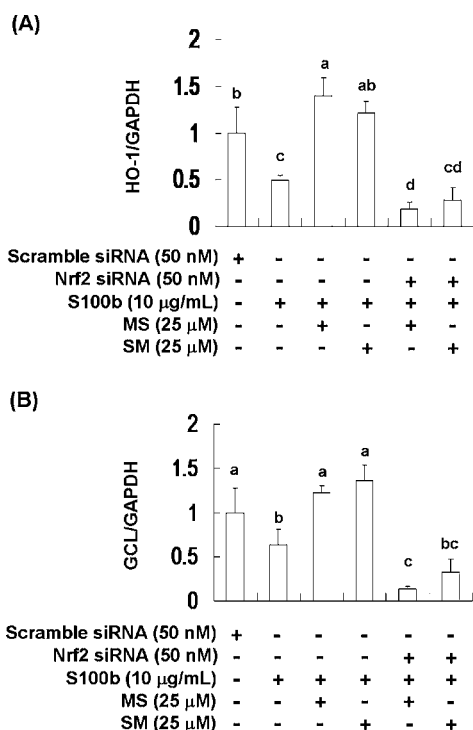


**Figure 7.** Effects of Nrf2 knockdown on antioxidant enzyme expression in S100b-treated THP-1 monocytes. Nrf2-knockdown-THP-1 cells were treated by S100b (10 µg/mL) with or without monascin (MS; 25 µM) and silymarin (SM; 25 µM) for 8 h, and then (A) HO-1 and (B) GCL mRNA expressions were measured by real-time PCR. Data are shown as the mean  $\pm$  SD ( $n = 3$ ). Significant differences are indicated by different letters ( $p < 0.05$ ).

metabolic disorder. Chronic poor control of blood glucose in diabetic patients can facilitate the glycation process and the accumulation of AGEs inside the body, thus triggering

complications of diabetes. AGEs can be covalently linked to intracellular proteins, lipids, and nucleic acids, affecting their structures and functions. This, in turn, leads to the decline of the overall function of tissues and organs, resulting in pathogenesis and aging of the body.<sup>5</sup>

Abnormal cellular accumulation of MG occurs invariably in diabetes.<sup>19</sup> MG decreases glucose tolerance in rodents,<sup>38</sup> suggesting that postprandial MG production in normoglycemic individuals could result in glucose intolerance and consequently greater MG accumulation. Glyoxal and MG as well as glucose are glycation agents that generate AGEs.<sup>5</sup> An in vitro antiprotein glycation assay has been used to search for glycation inhibitors to reduce production of AGEs.<sup>39</sup> Considerable effort has been made to identify clinically useful inhibitors of protein AGEs that delay or prevent glycation and ultimately alleviate insulin resistance.<sup>15</sup> These inhibitors include silymarin,<sup>11</sup> alagebrium,<sup>40</sup> quercetin,<sup>9</sup> and rutin.<sup>41</sup> In addition, AGE concentration in tissues shows a positive correlation with the severity of atherosclerotic lesions as well as levels of plasma proteins, lipoproteins, accumulated lipids, and VCAM-1 expression on the vascular wall or monocytes/macrophages; therefore, AGEs may play an important role in the formation of atherosclerosis.<sup>5</sup>

AGEs may transduce signals by interacting with RAGE. The interaction of AGEs with RAGE results in oxidative stress via activation of NADPH oxidase and mitochondrial oxidative pathways. This activation increases the production of a host of inflammatory molecules and molecules that provoke tissue injury.<sup>5</sup> The mechanisms by which antioxidants attenuate insulin resistance by suppressing immunocyte inflammation have been investigated.<sup>11,42</sup> Downstream signaling from RAGE to p47phox (a NADPH oxidase subunit) plays a role in the pathogenesis of alcoholic liver steatosis and inflammation-mediated oxidative stress; in this same study, p47phox deficiency prevented NFκB activation.<sup>11</sup>

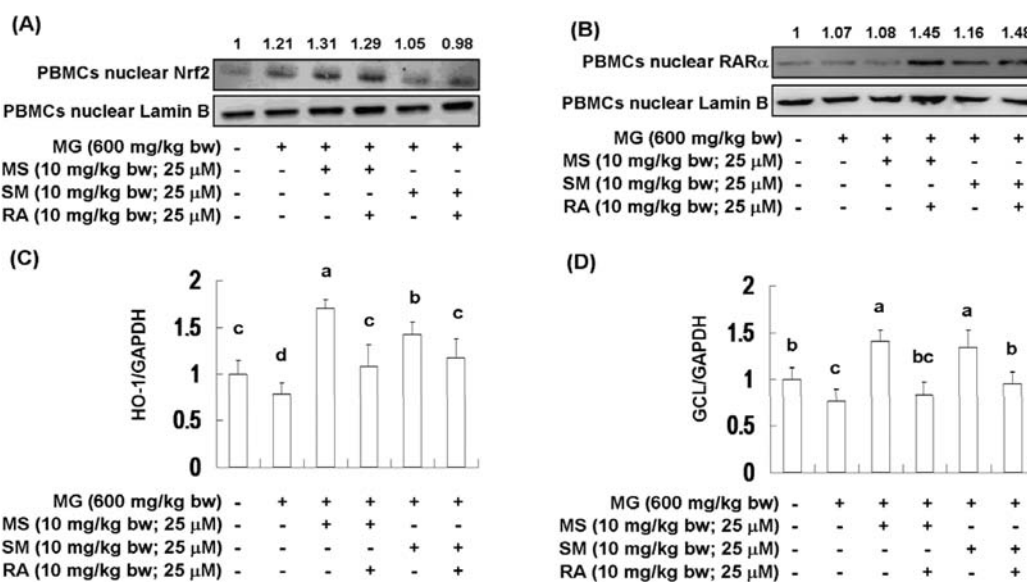


**Figure 8.** Activation of Nrf2 in PBMCs of methylglyoxal-induced rats. Effects of monascin (MS; 10 mg/kg bw), silymarin (SM; 10 mg/kg bw), and retinoic acid (RA; 10 mg/kg bw) on Nrf2 signaling molecules in PBMCs of methylglyoxal (MG; 600 mg/kg bw)-induced rats were investigated. After sacrifice, blood was collected and red blood cells (RBC) were removed by RBC lysis buffer, and then PBMCs was collected and treated with MS (25 µM), SM (25 µM), or RA (25 µM) for 8 h. Subsequently, (A) nuclear Nrf2 and (B) nuclear RARα were evaluated by Western blot. In addition, (C) HO-1 and (D) GCL mRNA in PBMCs treated with MS (25 µM), SM (25 µM), or RA (25 µM) for 8 h were investigated by real-time PCR. Data are shown as the mean  $\pm$  SD ( $n = 6$ ). Significant differences are indicated by different letters ( $p < 0.05$ ).

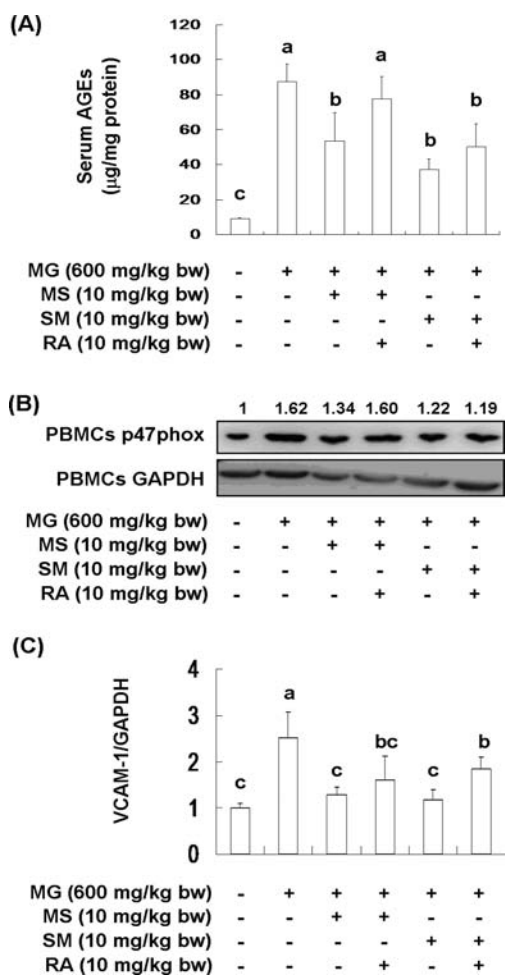


**Figure 9.** Effects of RAGE activation in PBMCs of methylglyoxal-induced rats. Effects of monascin (MS; 10 mg/kg bw), silymarin (SM; 10 mg/kg bw), and retinoic acid (RA; 10 mg/kg bw) on (A) serum AGEs level, (B) p47phox expression in PBMCs, and (C) VCAM-1 mRNA expression in PBMCs of methylglyoxal (MG; 600 mg/kg bw)-induced rats were investigated. After sacrifice, serum AGEs, p47phox of PBMCs, and VCAM-1 mRNA of PBMCs were measured. Data are shown as the mean  $\pm$  SD ( $n = 6$ ). Significant differences are indicated by different letters ( $p < 0.05$ ).

Several antioxidants, such as red grape juice, quercetin, and catechin, lower p47phox levels to prevent hypertension, endothelial dysfunction, and inflammation.<sup>43,44</sup> Moreover, Nrf2 activation can inhibit p47phox activity and reduce ROS and inflammation mediated by HO-1. We found that monascin and SM both suppressed oxidative stress caused by S100b induction in THP-1 monocytes to attenuate production of inflammatory factors (Figure 2). These effects were dependent on monascin, and SM inhibited p47phox translocation and NF $\kappa$ B activation (Figure 3).

SM possesses antioxidative activity, is hepatoprotective, and inhibits glycation.<sup>5,11</sup> Therefore, we treated rats with SM as a positive control. Phenolic compounds and antioxidants can promote Nrf2 activation, thereby reducing oxidative damage and insulin resistance in vitro and in vivo.<sup>11</sup> Moreover, Nrf2 plays an important role in improving glucose tolerance and insulin resistance in Nrf2-knockout mice fed a high-fat diet for 180 days.<sup>45</sup> Nrf2 activators can protect against renal damage in streptozotocin-induced diabetes and activate the protein kinase B signaling pathway to improve insulin sensitivity.<sup>46</sup> We found

that the ability of monascin to activate Nrf2 was greater than that of SM treatment in S100b-induced THP-1 monocytes (Figure 3). In addition, SM is an antioxidant that scavenges free radicals, avoiding oxidative stress;<sup>5,11</sup> but we have found that monascin cannot effectively scavenge DPPH free radical in a recent study.<sup>47</sup> These results revealed that monascin exerted antioxidation activity mediated by Nrf2, not through a direct free radical scavenging effect.

Hexose metabolism is known to generate excess MG and aldehydes in the liver, and these metabolites are detoxified by the sequential action of two thiol-dependent enzymes, (a) glyoxalase I, which catalyzes the formation of *S*-D-lactoylglutathione from 2-oxoaldehydes and GSH, and (b) glyoxalase II, which hydrolyzes thiol esters to produce D-lactate and GSH.<sup>5</sup> Furthermore, HO-1 protects against MG-treated insulin resistance, and its expression is suppressed by AGEs.<sup>48</sup> Notably, Nrf2 has been reported to up-regulate the expressions of glyoxalase and HO-1 in recent studies.<sup>46</sup> We found that monascin treatment significantly elevated the increases in HO-1 and GCL mRNA expression induced by S100b treatment in THP-1 monocytes (Figure 4). In addition, inhibition of serum AGEs by monascin administration was observed in MG-induced rats (Figure 9A), and this effect caused monascin to activate the hepatic glyoxalase system (data not shown). By contrast, we found that the inhibition of ROS level, TNF- $\alpha$ , and IL-1 $\beta$  production by monascin treatment was attenuated in S100b-induced THP-1 monocytes by Nrf2 siRNA knockdown (Figure 6). These results concerning the loss of anti-inflammatory effects correlated with HO-1 and GCL mRNA expression in Nrf2-knockdown THP-1 monocytes (Figure 7).

An in vivo study also revealed that Nrf2 inactivation markedly attenuated HO-1 and GCL expression in RA-induced rats by activating RAR $\alpha$ .<sup>24</sup> In the same study, evidence indicated that RAR $\alpha$  may bind to Nrf2, and this RAR $\alpha$ -Nrf2 complex subsequently reduced binding activity between Nrf2 and antioxidant response element (ARE) genes. We found that RA administration increased nuclear RAR $\alpha$  level in the PBMCs of MG-induced rats treated with RA for 8 h, thus interfering with HO-1 and GCL expression; however, monascin and SM both promoted HO-1 and GCL mRNA expression in PBMCs by activating Nrf2 (Figure 8).

On the basis of the concept that alteration of the albumin structure can result in impairments of its biological properties, bovine serum albumin was therefore utilized as a source of target proteins to evaluate the effects of phenolic acids on glycation. However, we found that monascin did not demonstrate antiglycative activity in a preliminary study (data not shown). To study the significance of glycoxidative stress on the pathology of diabetes, the effects of antioxidant supplements that inhibit protein modifications have been examined under diabetic conditions. These supplements have been hypothesized to be effective in treating complications of diabetes. This hypothesis is supported by clinical results indicating that the development of diabetes and accumulation of AGEs may be reduced by the intake of natural antioxidants through the diet. Therefore, the development and investigation of AGE inhibitors, especially natural anti-AGE agents that have few side effects, may yield a potential therapeutic approach for delaying and preventing premature aging and diabetic complications. We suggest that monascin is a novel antioxidant and Nrf2 activator that attenuates p47phox activation and inflammatory factor production and may prove to be an effective treatment for diabetes (Figure 9C).



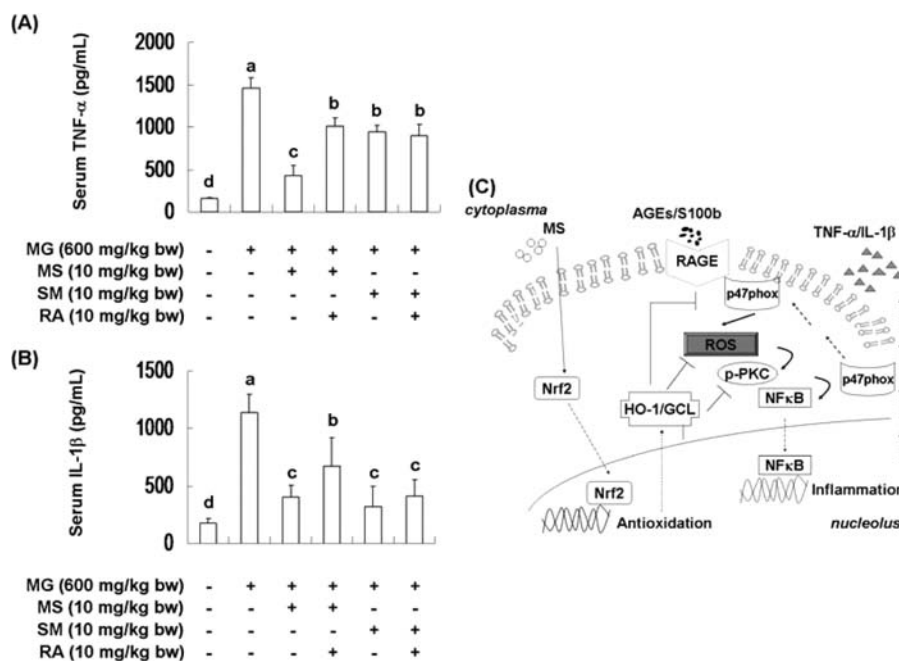


**Figure 10.** Potential mechanism of monascin on anti-inflammation. Effects of monascin (MS; 10 mg/kg bw), silymarin (SM; 10 mg/kg bw), and retinoic acid (RA; 10 mg/kg bw) on inflammatory cytokine production in methylglyoxal (MG; 600 mg/kg bw)-induced rats were investigated. Serum TNF- $\alpha$  (A) and IL-1 $\beta$  (B) of MG-induced rats were measured by ELISA kits. Data are shown as the mean  $\pm$  SD ( $n = 6$ ). Significant differences are indicated by different letters ( $p < 0.05$ ). (C) The potential mechanism of monascin (MS) attenuated inflammation caused by RAGE activation. MS promotes Nrf2 activation to elevate antioxidant status, thereby attenuating oxidative stress and inflammation caused by RAGE signal.

In addition, the relationship between MG and diabetes has been discussed in recent research.<sup>5</sup> However, in animal models, most studies still used streptozocin (STZ) to induce diabetes and then determined the level of MG in the serum. We consider that STZ-induced diabetes is through pancreatic  $\beta$  cell damage rather than through MG elevation. The direct effect and its action of MG on diabetes are still unclear. Our recent study found that 600 mg/kg bw MG treatment for 4 weeks could lead to obvious hyperglycemia and hyperinsulinemia in Wistar rats,<sup>49</sup> indicating that the dose in the study could be a good model for inducing diabetes, providing the reference for evaluating MG in the dietary-induced inflammation and diabetes in vivo in the future. This study clearly identified the dose of MG for diabetes induction, providing the reference to the level of MG in the diet for humans with abnormal blood glucose.

## ■ ASSOCIATED CONTENT

### 📄 Supporting Information

Supplementary Figure 1. This material is available free of charge via the Internet at <http://pubs.acs.org>.

## ■ AUTHOR INFORMATION

### Corresponding Author

\*Phone: +886-2-33664519, ext 10. Fax: +886-2-33663838. E-mail: [tspan@ntu.edu.tw](mailto:tspan@ntu.edu.tw).

### Funding

This research work and subsidiary spending were supported by the National Science Council (Taiwan) (NSC 99-2628-B-002-004-MY2).

### Notes

The authors declare no competing financial interest.

## ■ REFERENCES

- Day, J. F.; Thorpe, S. R.; Baynes, J. W. Nonenzymatically glycosylated albumin: in vitro preparation and isolation from normal human serum. *J. Biol. Chem.* **1979**, *254*, 595–597.
- Negre-Salvayre, A.; Salvayre, R.; Auge, N.; Pamplona, R.; Portero-Otin, M. Hyperglycemia and glycation in diabetic complications. *Antioxid. Redox Signal.* **2009**, *11*, 3071–3109.
- Schiekofer, S.; Andrassy, M.; Chen, J.; Rudofsky, G.; Schneider, J.; Wendt, T.; Stefan, N.; Humpert, P.; Fritsche, A.; Stumvoll, M.; Schleicher, E.; Haring, H. U.; Nawroth, P. P.; Bierhaus, A. Acute hyperglycemia causes intracellular formation of CML and activation of ras p42/44 MAPK and nuclear factor  $\kappa$ B in PBMCs. *Diabetes* **2003**, *52*, 621–633.
- Bonnefont-Rousselot, D. Glucose and reactive oxygen species. *Curr. Opin. Clin. Nutr. Metab. Care* **2002**, *5*, 561–568.
- Wu, C. H.; Huang, S. M.; Lin, J. A.; Yen, G. C. Inhibition of advanced glycation endproduct formation by foodstuffs. *Food Funct.* **2011**, *2*, 224–234.
- Wu, C. H.; Yeh, C. T.; Shih, P. H.; Yen, G. C. Dietary phenolic acids attenuate multiple stages of protein glycation and high-glucose-stimulated proinflammatory IL-1 $\beta$  activation by interfering with chromatin remodeling and transcription in monocytes. *Mol. Nutr. Food Res.* **2010**, *54*, 1–14.
- Wu, C. H.; Yen, G. C. Inhibitory effect of naturally occurring flavonoids on advanced glycation endproducts formation. *J. Agric. Food Chem.* **2005**, *53*, 3167–3173.
- Shanmugam, N.; Kim, Y. S.; Lanting, L.; Natarajan, R. Regulation of cyclooxygenase-2 expression in monocytes by ligation of the receptor for advanced glycation end products. *J. Biol. Chem.* **2003**, *278*, 34834–34844.
- Wang, J.; Chang, T. Methylglyoxal content in drinking coffee as a cytotoxic factor. *J. Food Sci.* **2010**, *75*, H167–H171.
- Adams, C. J.; Manley-Harris, M.; Molan, P. C. The origin of methylglyoxal in New Zealand manuka (*Leptospermum scoparium*) honey. *Carbohydr. Res.* **2009**, *344*, 1050–1053.
- Arribas-Lorenzo, G.; Morales, F. J. Analysis, distribution, and dietary exposure of glyoxal and methylglyoxal in cookies and their

relationship with other heat-induced contaminants. *J. Agric. Food Chem.* **2010**, *58*, 2966–2972.

(12) De Revel, G.; Bertrand, A. A method for the detection of carbonyl compounds in wine: glyoxal and methylglyoxal. *J. Sci. Food Agric.* **1993**, *61*, 267–272.

(13) Barros, A.; Rodrigues, J. A.; Almeida, P. J.; Oliva-Teles, M. T. Determination of glyoxal, methylglyoxal and diacetyl in selected beer and wine by HPLC with UV spectrophotometric detection after derivatization with *o*-phenyldiamine. *J. Liq. Chromatogr. Relat. Technol.* **1999**, *22*, 2061–2069.

(14) Khuhawar, M. Y.; Kandhro, A. J.; Khand, F. D. Liquid chromatographic determination of glyoxal and methylglyoxal from serum of diabetic patients using meso-stilbenediamine as derivatizing agent. *Anal. Lett.* **2006**, *39*, 2205–2215.

(15) Weng, C. J.; Chen, M. J.; Yeh, C. T.; Yen, G. C. Hepatoprotection of quercetin against oxidative stress by induction of metallothionein expression through activating MAPK and PI3K pathways and enhancing Nrf2 DNA-binding activity. *Nat. Biotechnol.* **2011**, *28*, 767–777.

(16) Yeh, C. T.; Yen, G. C. Induction of hepatic antioxidant enzymes by phenolic acids in rats is accompanied by increased levels of multidrug resistance-associated protein 3 mRNA expression. *J. Nutr.* **2006**, *136*, 11–15.

(17) Wu, C. H.; Huang, S. M.; Yen, G. C. Silymarin: a novel antioxidant with antiglycation and antiinflammatory properties in vitro and in vivo. *Antioxid. Redox Signal.* **2011**, *14*, 353–366.

(18) Huang, S. M.; Wu, C. H.; Yen, G. C. Effects of flavonoids on the expression of the pro-inflammatory response in human monocytes induced by ligation of the receptor for AGEs. *Mol. Nutr. Food Res.* **2006**, *50*, 1129–1139.

(19) Venugopal, S. K.; Devaraj, S.; Yang, T.; Jialal, I.  $\alpha$ -Tocopherol decreases superoxide anion release in human monocytes under hyperglycemic conditions via inhibition of protein kinase C- $\alpha$ . *Diabetes* **2002**, *51*, 3049–3054.

(20) Ramasamy, R.; Vannucci, S. J.; Du-Yan, S. S.; Herold, K.; Yan, S. F.; Schmidt, A. M. Advanced glycation end products and RAGE: a common thread in aging, diabetes, neurodegeneration, and inflammation. *Glycobiology* **2005**, *15*, 16–28.

(21) Lin, J. A.; Fang, S. C.; Wu, C. H.; Huang, S. M.; Yen, G. C. Anti-inflammatory effect of the 5,7,4'-trihydroxy-6-geranylflavanone isolated from the fruit of *Artocarpus communis* in S100B-induced human monocytes. *J. Agric. Food Chem.* **2011**, *59*, 105–111.

(22) Fukami, K.; Ueda, S.; Yamagishi, S. I.; Kato, S.; Inagaki, Y.; Takeuchi, M.; Motomiya, Y.; Bucala, R.; Iida, S.; Tamaki, K.; Imaizumi, T.; Cooper, M. E.; Okuda, S. AGEs activate mesangial TGF- $\beta$ -Smad signaling via an angiotensin II type I receptor interaction. *Kidney Int.* **2004**, *66*, 2137–2147.

(23) Spinetti, G.; Kraenkel, N.; Emanuelli, C.; Madeddu, P. Diabetes and vessel wall remodelling: from mechanistic insights to regenerative therapies. *Cardiovasc. Res.* **2008**, *78*, 265–273.

(24) Su, N. W.; Lin, Y. L.; Lee, M. H.; Ho, C. Y. Ankaflavin from *Monascus* fermented red rice exhibits selective cytotoxic effect and induces cell death on Hep G2 cells. *J. Agric. Food Chem.* **2005**, *53*, 1949–1954.

(25) Akihisa, T.; Tokuda, H.; Yasukawa, K.; Ukiya, M.; Kiyota, A.; Sakamoto, N.; Suzuki, T.; Tanabe, N.; Nishino, H. Azaphilones, furanoisophthalides, and amino acids from the extracts of *Monascus pilosus*-fermented rice (red-mold rice) and their chemopreventive effects. *J. Agric. Food Chem.* **2005**, *53*, 562–565.

(26) Martinkova, L.; Patakova-Juzlova, P.; Kren, V.; Kucerova, Z.; Havlicek, V.; Olsovsky, P.; Hovorka, O.; Rihova, B.; Vesely, D.; Vesela, D.; Ulrichova, J.; Prikrylova, V. Biological activities of oligo-ketide pigments of *Monascus purpureus*. *Food Addit. Contam.* **1999**, *16*, 15–24.

(27) Jou, P. C.; Ho, B. Y.; Hsu, Y. W.; Pan, T. M. The effect of *Monascus* secondary polyketide metabolites, monascin and ankaflavin, on adipogenesis and lipolysis activity in 3T3-L1. *J. Agric. Food Chem.* **2010**, *58*, 12703–12709.

(28) Lee, B. H.; Hsu, W. H.; Liao, T. H.; Pan, T. M. The *Monascus* metabolite monascin against TNF- $\alpha$ -induced insulin resistance via suppressing PPAR- $\gamma$  phosphorylation in C2C12 myotubes. *Food Chem. Toxicol.* **2011**, *49*, 2609–2617.

(29) Shi, Y. C.; Liao, V. H.; Pan, T. M. Monascin from red mold dioscorea as a novel antidiabetic and antioxidative stress agent in rats and *Caenorhabditis elegans*. *Free Radical Biol. Med.* **2012**, *52*, 109–117.

(30) Wang, X. J.; Hayes, J. D.; Henderson, C. J.; Wolf, C. R. Identification of retinoic acid as an inhibitor of transcription factor Nrf2 through activation of retinoic acid receptor  $\alpha$ . *Proc. Natl. Acad. Sci. U.S.A.* **2007**, *104*, 19589–19594.

(31) Hsu, Y. W.; Hsu, L. C.; Liang, Y. H.; Kuo, Y. H.; Pan, T. M. Monaphilones A-C, three new antiproliferative azaphilone derivatives from *Monascus purpureus* NTU 568. *J. Agric. Food Chem.* **2010**, *58*, 8211–8216.

(32) Lee, B. H.; Huang, Y. Y.; Wu, S. C. Hepatoprotective activity of fresh *Polygonum multiflorum* against Hep G2 hepatocarcinoma cell proliferation. *J. Food Drug Anal.* **2011**, *19*, 26–32.

(33) Figarola, J. L.; Shanmugam, K.; Natarajan, R.; Rahbar, S. Anti-inflammatory effects of the advanced glycation end product inhibitor LR-90 in human monocytes. *Diabetes* **2007**, *56*, 647–655.

(34) Ding, Y.; Kantarci, A.; Hasturk, H.; Trackman, P. C.; Malabanan, A.; Van Dyke, T. E. Activation of RAGE induces elevated O<sub>2</sub><sup>-</sup> generation by mononuclear phagocytes in diabetes. *J. Leukocyte Biol.* **2007**, *81*, 520–527.

(35) Kobayashi, A.; Ohta, T.; Yamamoto, M. Unique function of the Nrf2-Keap1 pathway in the inducible expression of antioxidant and detoxifying enzymes. *Methods Enzymol.* **2004**, *378*, 273–286.

(36) Hsu, W. H.; Lee, B. H.; Liao, T. H.; Pan, T. M. *Monascus*-fermented metabolite monascin suppresses inflammation via PPAR- $\gamma$  regulation and JNK inactivation in THP-1 monocytes. *Food Chem. Toxicol.* **2012**, *50*, 1178–1186.

(37) Hsu, W. H.; Lee, B. H.; Lu, I. J.; Pan, T. M. Ankaflavin and monascin regulate endothelial adhesion molecules and endothelial NO synthase (eNOS) expression induced by tumor necrosis factor- $\alpha$  (TNF- $\alpha$ ) in human umbilical vein endothelial cells (HUVECs). *J. Agric. Food Chem.* **2012**, *60*, 1666–1672.

(38) Ankrah, N. A.; Appiah-Opong, R. Toxicity of low levels of methylglyoxal: depletion of blood glutathione and adverse effect on glucose tolerance in mice. *Toxicol. Lett.* **1999**, *109*, 61–67.

(39) Brownlee, M. The pathological implications of protein glycation. *Clin. Invest. Med.* **1995**, *18*, 275–281.

(40) Dhar, A.; Desai, K. M.; Wu, L. Alagebrium attenuates acute methylglyoxal-induced glucose intolerance in Sprague-Dawley rats. *Br. J. Pharmacol.* **2010**, *159*, 166–175.

(41) Pashikanti, S.; deAlba, D. R.; Boissonneault, G. A.; Cervantes-Laurean, D. Rutin metabolites: novel inhibitors of nonoxidative advanced glycation end products. *Free Radical Biol. Med.* **2010**, *48*, 656–663.

(42) Ko, S. Y.; Lin, Y. P.; Lin, Y. S.; Chang, S. S. Advanced glycation end products enhance amyloid precursor protein expression by inducing reactive oxygen species. *Free Radical Biol. Med.* **2010**, *49*, 474–480.

(43) Dávalos, A.; de la Peña, G.; Sánchez-Martín, C. C.; Teresa Guerra, M.; Bartolomé, B.; Lasunción, M. A. Effects of red grape juice polyphenols in NADPH oxidase subunit expression in human neutrophils and mononuclear blood cells. *Br. J. Nutr.* **2009**, *102*, 1125–1135.

(44) Redondo, A.; Estrella, N.; Lorenzo, A. G.; Cruzado, M.; Castro, C. Quercetin and catechin synergistically inhibit angiotensin II-induced redox-dependent signalling pathways in vascular smooth muscle cells from hypertensive rats. *Free Radical Res.* **2012**, *46*, 619–627.

(45) Chartoumpakis, D. V.; Ziros, P. G.; Psyrogiannis, A. I.; Papavassiliou, A. G.; Kyriazopoulou, V. E.; Sykiotis, G. P.; Habeos, I. G. Nrf2 represses FGF21 during long-term high-fat diet-induced obesity in mice. *Diabetes* **2011**, *60*, 2465–2473.

(46) Zheng, H. T.; Whitman, S. A.; Wu, W.; Wondrak, G. T.; Wong, P. K.; Fang, D. Therapeutic potential of Nrf2 activators in

streptozotocin-induced diabetic nephropathy. *Diabetes* **2011**, *60*, 3055–3066.

(47) Lee, C. L.; Hung, H. K.; Wang, J. J.; Pan, T. M. Red mold dioscorea has greater hypolipidemic and antiatherosclerotic effect than traditional red mold rice and unfermented dioscorea in hamsters. *J. Agric. Food Chem.* **2007**, *55*, 7162–7169.

(48) He, M.; Siow, R. C.; Sugden, D.; Gao, L.; Cheng, X.; Mann, G. E. Induction of HO-1 and redox signaling in endothelial cells by advanced glycation end products: a role for Nrf2 in vascular protection in diabetes. *Nutr. Metab. Cardiovasc. Dis.* **2011**, *21*, 277–285.

(49) Lee, B. H.; Hsu, W. H.; Chang, Y. Y.; Kuo, H. F.; Hsu, Y. W.; Pan, T. M. Ankaflavin: a natural novel PPAR $\gamma$  agonist upregulates Nrf2 to attenuate methylglyoxal-induced diabetes *in vivo*. *Free Radical Biol. Med.* **2012**, *53*, 2008–2016.